Improvement of waste-fed bioelectrochemical system performance by selected electro-active microbes: Process evaluation and a kinetic study

László Koók, Nicolett Kanyó, Fruzsina Dévényi, Péter Bakonyi*, Tamás Rózsenberszki, Katalin Bélafi-Bakó, Nándor Nemestóthy

Research Institute on Bioengineering, Membrane Technology and Energetics, University of Pannonia, Egyetem u. 10, 8200 Veszprém, Hungary

*Corresponding Author: Péter Bakonyi
Tel: +36 88 624385
Fax: +36 88 624292
E-mail: bakonyip@almos.uni-pannon.hu

Abstract

In this work, bioaugmentation strategy was tested to enhance electricity production efficiency from municipal waste liquor feedstock in microbial fuel cells (MFC). During the experiments, MFCs inoculated with a mixed anaerobic consortium were enriched by several pure, electro-active bacterial cultures (such as *Propionibacterium freudenreichii*, *Cupriavidus basilensis* and *Lactococcus lactis*) and behaviours were assessed kinetically. It turned out that energy yield could be enhanced mainly at high substrate loadings. Furthermore, energy production and COD removal rate showed an optimum and could be characterized by a saturation range within the applied COD loadings, which could be elucidated applying the Monod-model for describing intracellular losses. Polarization measurements showed the positive effect of bioaugmentation also on extracellular losses. The data indicated a successful augmentation process for enhancing MFC efficiency, which was utmost in case of augmentation strain of *Propionibacterium freudenreichii*.

Keywords: bioaugmentation, microbial fuel cell, *Propionibacterium freudenreichii*, *Cupriavidus basilensis*, *Lactococcus lactis*

1. Introduction

Microbial fuel cell (MFC) technology can be considered as a rapidly developing alternative for generating electricity using electro-active microorganisms from the chemical energy stored in organic substrates [1 – 3]. As various research works demonstrated, besides easy-degradable materials, waste streams may also be utilized in MFCs as feedstock for electricity production [4, 5] e. g. synthetic human blackwater [6], industrial wastewaters [7 – 9], landfill leachate [10] or municipal solid waste [11]. Although in practice MFCs are typically operated with a mixed consortium in the anode chamber, a considerable number of pure cultures have been also tested including different Gram-negative/Gram-positive bacteria, yeasts and algae [12, 13]. In general, such single-strain MFCs are suitable for fundamental research and have limitations for real-field applications due to strict sterility requirements. Nevertheless, they can be viewed as potential candidates for the augmentation of mixed culture MFCs.

Bioaugmentation is a well-known strategy for process enhancement (i.e. aiming at the efficient removal of specific components) and relies on the addition of selected microbial species to an initial – mostly natural – microbial consortia/environment [14, 15]. The target compounds to be converted vary widely and can include oil-based contaminations, polycyclic aromatic hydrocarbons (PAHs), phenol, etc. according to the scientific literature [16 – 18]. Moreover, microbial augmentation can be advantageous not only in terms of specific substrate degradation but also to improve biofuel (e. g. biogas or biohydrogen) formation as well as integrated applications designed by coupling fermentation and bioelectrochemical treatment [19, 20]. The bioaugmentation in microbiologically-assisted electrochemical systems has been demonstrated with success (i.e. to utilize corn stover [21] or synthetic wastewater [22]) by exploiting specific syntrophic processes and hierarchical structures present in such systems in order to boost electricity generation [23]. So far, electro-kinetic analysis of MFCs augmented with *Shewanella haliotis*

[22] showed the positive effect of this technique on the grounds of power output and substrate biodegradation. The observed benefits could be mainly attributed to lower activation losses and enhanced shuttling between redox intermediates [22]. In another paper applying electro-active *Pseudomonas aeruginosa* and non-electro-active *Escherichia coli* strains for bioaugmentation in MFCs, it could be concluded that the bioelectrochemical cells had taken advantage of synergistic species interactions in the mixed consortia, leading to lower polarization resistance and increased power generation capacity [24].

In this work, bioaugmentation of MFCs was carried out by employing pure isolates of electro-active bacteria, namely *Propionibacterium freudenreichii*, *Cupriavidus basilensis* and *Lactococcus lactis*, which to our knowledge, have not been used for this this purpose. *P. freudenreichii* is a Gram-positive obligate anaerobic bacteria belonging to the phylum *Actinobacteria* and known as an endogenous mediator-producing strain. Actually, 1,4-dihydroxy-2-naphthoic acid (DHNA) and 2-amino-3-dicarboxy-1,4-naphthoquinone (ACNQ) are reported as electron shuttle molecules, secreted by *P. freudenreichii* [25, 26] which allow its application in mediator-less MFC systems [27]. *C. basilensis* is a flagellated Gram-negative, facultative aerobic β-*proteobacteria* [28] and able to the utilize substances e.g. phenol or aliphatic alcohols as substrates [29, 30]. The members of this genus are described to be capable of producing endogenous mediators for extracellular electron transfer [30, 31]. Since *C. basilensis* is metal-resistant and able to degrade a wide range of materials, its use seems to be promising in wastewater treatment as well as in bioelectrochemical technologies. *L. lactis*, a member of phylum *Firmicutes*, is a Gram-positive, facultative anaerobic bacterium with a potential as a biocatalyst in microbial electrochemical cells because of its self-secreted electron accepting and shuttling agent, ACNQ [32, 33]. Furthermore, its important trait is the capability of pursuing electrochemically-modified metabolic pathway besides homolactic fermentation, which leads to the formation of acetate (as by-product) to be

consumed by other i.e. exoelectrogenic microorganisms present in an augmented bioelectrochemical reactor [33].

To our best knowledge, no comparative study has been done yet with these microbes to investigate bioaugmentation process in MFCs that involves a kinetic approach for the assessment of system behaviour in the course of waste utilization. Therefore, the results demonstrated may have novelty and added-value to support the better understanding of bioaugmentation in MFCs and expand the perspectives of such bioelectrochemical cells.

2. Materials and methods

2.1. Seed source and substrates

For MFC inoculation, seed source was collected from beet pulp utilizing biogas fermentation unit of Hungarian sugar factory, located at Kaposvár, with an initial microbial community structure demonstrated in our recent work [34]. The anaerobic sludge was pretreated (starved) in a laboratory-scale reactor before use for one week at 37 °C. Its main characteristics were the followings: COD content: 12 g L^{-1}, pH = 7.8, Total solids: 6.7 %. As for substrate, pressed fraction of municipal solid waste (LPW) was used. Characteristics of LPW can be found in previous publications [11, 35 – 37]. The most important parameters of the substrate and the flow diagram of its preparation process can be seen in **Fig. 1.**

2.2. Preparation of pure cultures of selected electro-active microbes for bioaugmentation

The pure cultures of selected microbes were purchased from the German Collection of Microorganisms and Cell Cultures (DSMZ). The broth media compositions were the followings: *Lactococcus lactis* (DSMZ-20481) broth – casein peptone (pancreatic digest) 17 g L^{-1}, K_2HPO_4 2.5 g L^{-1}, glucose 2.5 g L^{-1}, NaCl 2.5 g L^{-1}, soy peptone (papaic digest) 3 g L^{-1}, yeast extract 3 g L^{-1}, agar 20 g L^{-1} (pH = 7); *Cupriavidus basilensis* (DSMZ-11853) broth – peptone 5 g L^{-1}, meat extract 3 g L^{-1}, agar 20 g L^{-1} (pH = 7); *Propionibacterium freudenreichii* (DSMZ-20271) broth – casein peptone (tryptic digest) 10 g L^{-1}, yeast extract 5 g L^{-1}, Na-lactate 10 g L^{-1}, agar 20 g L^{-1} (pH = 7).

The cultures were incubated on agar plates – and in stab agar in case of *P. freudenreichii* – for two days at 37 °C. Thereafter, colonies were harvested and transferred to liquid media (50 mL, without agar) and incubated for two more days under the same conditions. Before use in MFCs, the cell concentration of liquid cultures was determined by Bürker's chamber.

2.3. MFC design and setup

The design of dual-chamber microbial fuel cells was adopted from our previous work [38]. In this MFC construction, anode and cathode compartments (with 60 mL total volume) were equipped with carbon cloth (Zoltek Corp., USA) and Pt-C (0.3 mg cm^2 Pt content, FuelCellsEtc, USA) electrodes (64 cm^2 apparent surface area), respectively. The anode and cathode were connected by Ti wire (Sigma-Aldrich, USA) to the external circuit, containing a 100 Ω resistor. The chambers were separated by Nafion 115 proton exchange membrane (Sigma-Aldrich, USA) with diameter of 4.5 cm. Before use, the membrane was activated as described elsewhere [38]. In order to maintain aerobic conditions, air was continuously supplemented to the cathode compartment.

The anode side of MFCs was filled with 50 mL of mesophilic sludge (pH adjusted to 7) and 5 mL of individual, pure strain liquid culture. Based on cell counting and prior to loading, the liquid cultures were diluted to provide equal cell concentration for each bioaugmented reactors. Thus, initial cell concentration of 3.23 x 10^7 ± 2.6 x 10^6 cells mL^{-1} could be reached and maintained in the liquid (5 mL) samples employed for bioaugmentation, irrespective of the strain. The anode chamber was then purged with high purity nitrogen gas to remove dissolved oxygen and ensure anaerobic conditions. In the cathode chamber, 50 mM phosphate buffer (pH = 7) was used as electrolyte. The MFC reactors were running at 37 °C. In addition to the bioaugmented reactors, control MFCs started-up only with (55 mL) inoculum (50 mL sleed sludge + 5 mL phosphate buffer) was established, as well. Substrate (LPW, Section 2.1.) additions (0.5, 1, 2 and 4 mL, depending on the aimed COD loading) were carried out by using batch operational mode, after the adaptation phase has been successfully performed (Section 3.1.). During each injection of LPW, the appropriate amount of anolyte was drawn (exchange of volumes) to ensure a consistent working volume. Once the observed voltage dropped close to the initial (**Fig. 2**), a new feeding cycle could be commenced [34].

2.4. Analysis and calculations

Cell voltage (U) was measured and monitored through a 100 Ω external resistor by a data acquisition system (National Instruments, USA) in Labview environment. According to Ohm's law, current (I) (and electric power, P) were computed. Cell polarization measurements were carried out by varying the resistors in the external circuit of MFCs between 3.3 kΩ – 10 Ω. From the linear region of voltage vs. polarization current density ($i_{max,P}$) plots, the overall internal cell resistance (R_i) – as the slope of the fitted trendline – could be derived.

The energy yield was calculated according to Eq. 1:

$$Y_S = \frac{E}{m_{\Delta COD}\, A} \quad (1)$$

where A is the apparent anode surface area (m^2), E is the cumulated energy (kJ) derived from the integration of P – t curves, $m_{\Delta COD}$ is the quantity of COD removed (gram) during a given cycle. The COD content of particular samples was analyzed in accordance with our previous paper [39] by relying on the standard methods of APHA.

The rates of (i) Energy production and (ii) COD removal were computed according to Eqs. 2 and 3, respectively, considering the operation time of given batch cycles (τ):

$$v_E = \frac{E}{A\,\tau} \quad (2)$$

$$v_S = \frac{m_{\Delta COD}}{V\,\tau} \quad (3)$$

The effect of substrate concentration on current generation – and thus, intracellular losses – was evaluated by adopting the principles of Monod model [40]. In this model the relation of the two variables (substrate concentration and current density) can be described by Eq. 4.

$$i = i_{max} \frac{[S]}{K_{S,app}+[S]} \quad (4)$$

where i denotes the current density (relative to the apparent anode surface area), $K_{S,app}$ is the apparent half-saturation substrate concentration (half-saturation constant) and [S] is the substrate (LPW) concentration. To estimate the kinetic parameters (i_{max} and $K_{S,app}$) the linearized (double-reciprocal) form of Eq. 4 was applied, as represented in Eq. 5.

$$\frac{1}{i} = \frac{K_{S,app}}{i_{max}[S]} + \frac{1}{i_{max}} \quad (5)$$

In the model (Eqs. 4 and 5), [*S*] is given in the unit of e^- eq L^{-1}, considering 8 g COD as equivalent of 1 mol e^- [40].

The determination of mean values and standard deviations/errors for parameters such as i_{max}, $P_{d,max}$, Y_S, v_S, v_E, etc. appearing throughout this work (i.e. **Table 1**) was carried out as detailed in the Supplementary file (**Fig. 1S**).

3. Results and Discussion

3.1. Evaluation of bioaugmentation efficiency in MFC – peak current and power densities, energy yield

In the first part of operation – considered as the acclimation period – 5 mM acetate was added in the MFCs as adapting substrate in consecutive cycles until comparable current density profiles in particular reactors were reached over time (after three weeks) [41]. Afterwards, feeding of stabilized MFCs was commenced with LPW and the measurements were dedicated to examine the impact of bioaugmentation. The MFCs were operated with different amounts of LPW in the range of 0.5 – 4 mL (equivalent to 0.88 – 7.04 g_{COD} L^{-1}). The most important parameters of each system tested are summarized in **Table 1** (average output values and standard deviations for the individual feeding processes) and the current density profiles can be seen in **Fig. 2**.

In terms of highest attainable current and power densities (noticed at the highest LPW supplementation, 7.04 g_{COD} L^{-1}), the MFCs could be ranked in the following order: *Propionibacterium*-MFC (76.2 – 110.3 mA m^{-2} / 3.7 – 7.8 mW m^{-2}, respectively), *Cupriavidus*-MFC (70.6 – 100.1 mA m^{-2} / 3.2 – 6.4 mW m^{-2}), Control-MFC (66.2 – 102 mA m^{-2} / 2.8 – 6.7 mW m^{-2}) and *Lactococcus*-MFC (57.6 – 95.1 mA m^{-2} / 2.1 – 5.8 mW m^{-2}). Interestingly, in the light of already published literature relevant to the latest strain, *L. lactis*, though Freguia et al.

[33] achieved proper operation of MFCs using its monoculture to generate current from glucose, no electrogenic activity in MFCs was found by Rosenbaum et al. [42] with *L. lactis* alone on the same substrate. Interestingly, however, co-cultures of *Shewanella oneidensis* and *L. lactis* were able to produce current (64 – 215 mA m^{-2}) from this substance [42]. Hence, it can be implied that the behaviour of *L. lactis* is dependent on factors such as the composition of underlying community structure (i.e. the number and features of other bacteria to live and cooperate with), which is likely true for *C. basilensis and P. freudenreichii* as well. To assess such aspects (i.e. how the microbiological background of the sludge inoculum influences the integration of particular cultures into the community) the population dynamics should be tracked via molecular biological tools, which should be the subject of a follow-up study.

Ys, as expressed in Eq. 1, is an appropriate response variable to make comparison between the systems from the point of view of cumulative energy recovery efficiency. According to the results, an LPW (substrate) concentration-dependent variation of Ys was found in all cases, where at low COD loadings (0.88 and 1.76 g_{COD} L^{-1}) only the *Cupriavidus*-MFC could surpass the Control-MFC. In case of *Propioni*-, *Cupriavidus*- and Control-MFCs, nearly equal energy yields (1.59, 1.62 and 1.69 kJ $g_{\Delta COD}^{-1}$ m^{-2}, respectively) could be observed at middle COD loading of 3.52 g_{COD} L^{-1}. Nevertheless, by further increasing the COD loading to the highest value of 7.04 g_{COD} L^{-1}, energy yields were significantly improved in all bioaugmented MFCs in comparison with the Control-MFC. As a matter of fact, increment of *Ys* relative to the control reactor was 91 %, 47 % and 21 % for *Propioni*-, *Lactococcus*- and *Cupriavidus*-MFCs, respectively (**Table 1**).

Overall, from the process evaluation considering peak current and power densities as well as energy yield, it would appear that the obligate anaerobic *P. freudenreichii* was the most promising among the strains for augmentation under the experimental circumstances provided.

3.2. On energy production and COD removal rates

Trends of Coulombic efficiency (CE) (derived in accordance with Logan et al. [3] considering the amount of COD removed) as a function of COD loading can be observed in **Fig. 3**, which implies that bioaugmentation had an advantageous effect on CE at every operating point. The difference between CEs was less pronounced at the lowest COD loading where CE obtained to be about 1.3 – 1.8 %. Nevertheless, by increasing the COD loading, the increment in CE values of the augmented MFCs became more and more emphasized compared to the control and by reaching the highest loading (7.04 g_{COD} L^{-1}), the *Propionibacterium*-, *Cupriavidus*- and *Lactococcus*-MFC exceeded the CE of Control-MFC by 129, 35 and 50 % (with corresponding CEs of 3.88 ± 0.21 %, 2.28 ± 0.1 % and 2.52 ± 0.14 % versus 1.69 ± 0.12 %), respectively. CEs in the same order of magnitude had been obtained in our previous work, demonstrating a sequential anaerobic treatment process (biohydrogen fermentation – biogas generation – microbial fuel cell) for the enhancement of overall energy recovery from LPW as feedstock [37].

To assess the MFC efficiency, not only the total achievable energy yields (product) and COD (substrate) removals are to be considered but corresponding rates as well since the process should be accomplished within a reasonable time. Consequently, an evaluation based on reaction rate-like variables defined in Eqs. 2 and 3 is of importance.

As it is depicted in **Fig. 4**, similar relationship could be established between energy production rate (ν_E) and COD loadings for all MFCs until 3.52 g_{COD} L^{-1} concentration. However, at the highest COD dose (7.04 g_{COD} L^{-1}), ν_E in the bioaugmented cells was declined and hence, a peak ν_E value could be noted within the COD range investigated. The phenomena that decreased ν_E was observed in case of bioaugmented cells at 7.04 g_{COD} L^{-1} (than at 3.52 g_{COD} L^{-1}) is attributed to the nonlinear increase of operation times for batch cycles. It is also to notice in **Fig. 4** that there was a considerable difference of ν_E between the systems at 3.52 g_{COD} L^{-1} concentration, leading to a 47 % faster

energy recovery rate by the most efficient *Propionibacterium*-MFC compared to the control (non-bioaugmented) reactor (482 and 327 J m^{-2} d^{-1}, respectively). However, at highest COD addition (7.04 g_{COD} L^{-1}), more or less similar ν_E was found for all MFCs This suggests the existence of substrate (COD) saturation range where although more organic matter is available, the reaction rate is not further enhanced in a proportional way due to fully exploited capacity of exoelectrogens present in MFCs. A basically similar discussion can be mead concerning the data related to COD (substrate) removal rates (ν_S), as illustrated in **Fig. 5**. The fact that tendencies in ν_E and ν_S are analogous can be explained by concurrent product (energy) formation and substrate (COD in LPW feedstock) consumption. In essence, at 3.52 g_{COD} L^{-1}, the maximum ν_S was attained with the *Propionibacterium*-MFC, being 31 % higher than for the Control-MFC (5.52 and 4.2 g L^{-1} d^{-1}, respectively). The ν_S values (between 1 – 5.52 g L^{-1} d^{-1}, depending on the actual COD loading) are comparable to the relevant literature, where for example Raghavulu et al. [22] demonstrated ν_S of 0.41 g L^{-1} d^{-1} by using *S. haliotis* as augmentation species. In another publication, ν_S of 0.59 g L^{-1} d^{-1} could be reached with *P. aeruginosa*-augmented MFCs, which was 11 % greater than the non-augmented system demonstrating ν_S = 0.53 g L^{-1} d^{-1} [24]. Moreover, phenol-utilizing (pure culture) *C. basilensis*-MFC could be characterized by roughly one order of magnitude lower COD removal rate ($\nu_S \approx$ 0.05 g L^{-1} d^{-1}) [32].

It is noteworthy that ν_E and ν_S are representative for a whole batch cycle, during which, however, various stages of both product formation and substrate removal can be distinguished. These, in particular, include consecutive phases of (i) increasing, (ii) maximal (steady-state) and (iii) decreasing current production and simultaneous COD elimination rates. Among them, the main point of interest is the steady-state with maximal (i) current production and (ii) substrate utilization rates, where various intra- and extracellular mechanism/factors play a role [40]. Thus, in the next sections, the MFC data collected under steady-state conditions will be processed. Firstly (Section

334 3.3.), a kinetic approach will be applied to get an insight to intracellular losses
335 related to reaction rate and bioconversion capacity of exoelectrogens [40].
336 Secondly (Section 3.4.), polarization results will be presented to evaluate
337 extracellular losses [40].
338

3.3. Monod model for substrate utilization kinetics – intracellular losses

The current generation and its kinetics are determined by two main factors at intracellular level (where the electrons are conveyed from the electron donor molecule to the outer membrane proteins or secreted shuttle molecules) [40]. Firstly, substrate degradation takes place and reduced intracellular charge carrier molecules (NADH) are formed [43]. Afterwards, processes with the involvement of electron transport chain govern the electrons to the starting point of extracellular electron transfer. The former step can be described by the Monod model (Eq. 4), which correlates the current density with substrate concentration [43]. Therefore, plotting maximal (steady-state) current densities vs. substrate concentration allows studying related (intracellular) energy losses. It is to note that experimental results obtained at 0.44 g_{COD} L^{-1} were added to make the analysis via the Monod model more reliable. The double-reciprocal interpretation (Eq. 5) of Monod model is depicted in **Fig. 6.** Based on the slope of trendlines fitted for the bioaugmented and non-bioagumented (control) MFCs, kinetic parameters (i_{max} and $K_{S,app}$) could be delivered. As it can be drawn from **Table 2**, comparable i_{max} values were found for all systems (109.9-120.5 mA m^{-2}). This, together with **Fig. 7** confirms the implications made in Section 3.3. regarding the existence of a substrate saturation range where the highest COD loading (7.04 g_{COD} L^{-1}, which is 882 e^- meq L^{-1} according to Eq. 5) belongs to. As for $K_{S,app}$ listed in **Table 2***,* the MFC augmented with *P. freudenreichii* demonstrated the lowest value with 67.7 e^- meq L^{-1}, followed by *C. basilensis*-MFC (73.5 e^- meq L^{-1}), Control-MFC (91 e^- meq L^{-1}) and *Lactococcus*-MFC (99.4 e^- meq L^{-1}). In essence, obtaining a lower $K_{S,app}$ is advantageous from a reaction rate point of view. Thus, the energy production rate (ν_E) achieved in *Propionibacterium*-MFC (compared to the other reactors) can be likely associated with the low $K_{S,app}$ value, helping to maintain relatively higher electricity generation even at lower substrate (COD) concentrations in accordance with the Monod model (zero-order kinetics). Overall, bioaugmentation with the aid of selected pure

bacterial cultures such as *P. freudenreichii* and *C. basilensis* could effectively decrease the limiting substrate concentration in MFCs. Once high (close to maximal) ν_E is kept at lower [*S*], the intracellular losses ascribed to the only partly exploited capacity of active exoelectrogens (causing limitation of reaction rate) in MFC can be reduced [40].

In fact, $K_{S,app}$ and i_{max} values obtained in this work are somewhat lower compared to other MFC research studies using components such as acetate, ethanol or propionate, probably due to the complex structure of LPW feedstock. For instance, $K_{S,app}$ = 19 e^- meq L^{-1} (i_{max} = 2200 mA m^{-2}) was observed in case of acetate-utilizing MFC [45]. In another work, $K_{S,app}$ = 0.18 - 58 e^- meq L^{-1} was documented for ethanol substrate [46]. In microbial electrolysis cell (MEC) mode, Torres et al. [47] reported half-saturation constants of 22, 5.3 and 3.8 e^- meq L^{-1} for acetate, ethanol and propionate, respectively, while maximal current densities varied between approximately 1.8 – 9 A m^{-2}.

3.4. Cell polarization characteristics – extracellular losses

Basically, polarization techniques can be applied to describe the system from extracellular processes (and related potential or energy losses) [3]. These, on the anode side, cover (i) the transfer of electrons to the conductive biofilm matrix and/or soluble shuttle molecules in the bulk phase and (ii) the charge transport (conductive or diffusive) to the anode surface, where the electrode reaction takes place. By varying the external resistance in the MFC electrical circuit and measuring the cell voltage subsequently, polarization and power density curves (*U* vs. *i* and P_d vs. *i*, respectively) can be registered (**Fig. 8**). Based on these data, the actual internal resistance (R_i) of an MFC is estimated [3]. Considering the polarization chart (taken in steady-state at 7.04 g_{COD} L^{-1} LPW concentration), (i) activation polarization, (ii) ohmic and (iii) concentration polarization regions could be identified in each MFC. The open circuit voltages (OCV) were comparable, spanning 425 – 442 mV. As for R_i in

the bioaugmented MFCs, values belonging to *Lactococcus*-, *Propionibacterium*- and *Cupriavidus*-MFC were noted such as 347 Ω, 341 Ω and 348 Ω (with $R^2 > 0.98$). In the Control-MFC, the corresponding value was higher (383 Ω).

The comparable voltages occurring at low current densities (**Fig. 8**) can be explained by the restricted passage of electrons through the circuit, caused by high external resistor [44]. Therefore, from these similar values, a resistance value can be assumed above which the global reaction rate in MFC (ending with proton reduction at the cathode by electrons captured and delivered from the anode) will be independent of the microbial reduction rate of charge-carrying redox components. By lowering the external resistance, continuous voltage drop and simultaneously increasing current density can be observed, where more oxidized-form electron carriers are present and implicitly, the marked role of electro-active microbial metabolism becomes apparent. Moreover, *i* in various MFCs can be properly distinguished at lower (external) resistances, as indicated by **Fig. 8**. In general, the bioaugmented MFCs generated higher maximal polarization current density ($i_{max,P}$) than the Control-MFC did. Expressed in numbers, $i_{max,P}$ of 110, 116 and 127 mA m^{-2} could be reached in *Lactococcus*-, *Cupriavidus*- and *Propionibacterium*-MFCs, respectively, where the latest case demonstrates 21 % increment relative to the non-augmented system (105 mA m^{-2}).

The significantly positive effect of bioaugmentation on MFC performance could be recognized on grounds of maximal power densities ($P_{d,max}$, **Fig. 8**) to be ordered as follows: 6.6 mW m^{-2} (Control-MFC), 7.9 mW m^{-2} (*Cupriavidus*-MFC), 8.2 mW m^{-2} (*Lactococcus*-MFC), 9.8 mW m^{-2} (*Propionibacterium*-MFC). Thus, in this aspect too, the enrichment of microbial consortia by *P. freudenreichii* was the most advantageous strategy to improve bioelectrochemical system efficiency. The findings presented are in agreement with the literature, where Raghavulu et al. [22] attained OCV of 378 mV using *S. haliotis* for bioaugmentation with R_i, $i_{max,P}$ and $P_{d,max}$ of 300 Ω, 320 mA m^{-2} and 29.6 mW m^{-2}, respectively. In addition, bioaugmentation of MFCs with *P.*

aeruginosa resulted in relatively high OCV (418 mV) and maximal power density (69.9 mW m^{-2}) with polarization current density of ~ 450 mA m^{-2} [24]. The results of Reiche et al. [28] for *P. freudenreichii*-driven MFC are also comparable to ours with *Propionibacterium*-MFC, realizing OCV of 485 mV and $P_{d,max}$ of 14.9 mW m^{-2} [28]. In MFCs operated with monoculture of *C. basilensis* as exoelectrogenic biocatalyst, Friman et al. [32] could observe OCV of about 250 mV and $P_{d,max}$ of 10 mW m^{-2}, which coincide well with our values in *Cupriavidus*-MFC (OCV = 425 mV and $P_{d,max}$ = 7.9 mW m^{-2}).

In this work, the selected electro-active bacteria were known as producers of electron shuttle molecules (Section 1.) and therefore, a process via such soluble compounds can be supposed. This argument seems to be supported by the current density values documented in this investigation ($i_{max,P}$ in the order of 10^2 mA m^{-2}), implying the more likely occurrence of mediated (diffusion controlled) electron transport rather than a direct contact mechanism [40].

4. Conclusions

In this study, bioaugmentation process and its effect on microbial fuel cell performance were investigated by several electro-active bacterial cultures. Considering the electric outputs (i.e. current and power density) and energy yield, the bioaugmented MFCs were more efficient at higher COD loadings than the control. The analysis of energy production and COD removal rates revealed an optimum COD loading. Besides, substrate saturation and the existence of zero-order kinetics region at the highest substrate concentration were confirmed by applying Monod model. $K_{S,app}$ values could be significantly decreased in case of *Propinobacterium*- and *Cupriavidus*-MFC compared to the control. Polarization measurements indicated the positive impact of bioaugmentation on extracellular losses and enhanced electron shuttle mechanism could be presumed. In conclusion, microbial augmentation can be considered as a promising strategy to improve microbial fuel cells. After

examination of systems behavior from various points of views, *Propionibacterium freudenreichii* was found as the most advantageous strain among those tested for bioaugmentation in the experiments.

Acknowledgements

Péter Bakonyi acknowledges the support received from National Research, Development and Innovation Office (Hungary) under grant number PD 115640. The János Bolyai Research Scholarship of the Hungarian Academy of Sciences is duly acknowledged for the support. The “GINOP-2.3.2-15 – Excellence of strategic R+D workshops (Development of modular, mobile water treatment systems and waste water treatment technologies based on University of Pannonia to enhance growing dynamic export of Hungary (2016-2020))” is thanked for supporting this work. László Koók was supported by the ÚNKP-17-3 ‘‘New National Excellence Program of the Ministry of Human Capacities”.

References

[1] Allen, R. M., Bennetto, H. P., 1993. Microbial fuel-cells. Appl. Biochem. Biotechnol. 39, 27-40.

[2] Rabaey, K., Verstraete, W., 2005). Microbial fuel cells: novel biotechnology for energy generation. Trends Biotechnol. 23, 291-298.

[3] Logan, B.E., Hamelers, B., Rozendal, R., Schröder, U., Keller, J., Freguia, S., et al., 2006. Microbial fuel cells: methodology and technology. Environ. Sci. Technol. 40, 5181-5192.

[4] Pant, D., Van Bogaert, G., Diels, L., Vanbroekhoven, K., 2010. A review of the substrates used in microbial fuel cells (MFCs) for sustainable energy production. Bioresour. Technol. 101, 1533-1543.

[5] Pandey, P., Shinde, V.N., Deopurkar, R.L., Kale, S.P., Patil, S.A., Pant, D., 2016. Recent advances in the use of different substrates in microbial

fuel cells toward wastewater treatment and simultaneous energy recovery. Appl. Energy 168, 706-723.

[6] Vogl, A., Bischof, F., Wichern, M., 2016. Single chamber microbial fuel cells for high strength wastewater and blackwater treatment—A comparison of idealized wastewater, synthetic human blackwater, and diluted pig manure. Biochem. Eng. J. 115, 64-71.

[7] Dong, Y., Qu, Y., He, W., Du, Y., Liu, J., Han, X., Feng, Y., 2015. A 90-liter stackable baffled microbial fuel cell for brewery wastewater treatment based on energy self-sufficient mode. Bioresour. Technol. 195, 66-72.

[8] Fang, Z., Song, H. L., Cang, N., Li, X. N., 2015. Electricity production from Azo dye wastewater using a microbial fuel cell coupled constructed wetland operating under different operating conditions. Biosens. Bioelectron. 68, 135-141.

[9] Abbasi, U., Jin, W., Pervez, A., Bhatti, Z. A., Tariq, M., Shaheen, S., et al., 2016. Anaerobic microbial fuel cell treating combined industrial wastewater: Correlation of electricity generation with pollutants. Bioresour. Technol. 200, 1-7.

[10] Hassan, M., Pous, N., Xie, B., Colprim, J., Balaguer, M. D., Puig, S., 2017. Influence of iron species on integrated microbial fuel cell and electro-Fenton process treating landfill leachate. Chem. Eng. J. 328, 57-65.

[11] Koók, L., Rózsenberszki, T., Nemestóthy, N., Bélafi-Bakó, K., Bakonyi, P., 2016. Bioelectrochemical treatment of municipal waste liquor in microbial fuel cells for energy valorization. J. Clean. Prod. 112, 4406-4412.

[12] Logan, B.E., 2009. Exoelectrogenic bacteria that power microbial fuel cells. Nat. Rev. Microbiol. *7*, 375-381.

[13] Strik, D.P.B.T.B., Terlouw, H., Hamelers, H.V.M, Buisman, C.J.N, 2008. Renewable sustainable biocatalyzed electricity production in a

524 photosynthetic algal microbial fuel cell (PAMFC). Appl. Microbiol.
525 Biotechnol. 81, 659-668.
526 [14] Tyagi, M., da Fonseca, M. M. R., de Carvalho, C. C., 2011.
527 Bioaugmentation and biostimulation strategies to improve the
528 effectiveness of bioremediation processes. Biodegradation, 22, 231-241.
529 [15] Mrozik, A., Piotrowska-Seget, Z., 2010. Bioaugmentation as a strategy
530 for cleaning up of soils contaminated with aromatic
531 compounds. Microbiol. Res. 165, 363-375.
532 [16] Tahhan, R. A., Ammari, T. G., Goussous, S. J., Al-Shdaifat, H. I., 2011.
533 Enhancing the biodegradation of total petroleum hydrocarbons in oily
534 sludge by a modified bioaugmentation strategy. Int. Biodeterior.
535 Biodegradation. 65, 130-134.
536 [17] Sayara, T., Borràs, E., Caminal, G., Sarrà, M., Sánchez, A., 2011.
537 Bioremediation of PAHs-contaminated soil through composting:
538 influence of bioaugmentation and biostimulation on contaminant
539 biodegradation. Int. Biodeterior. Biodegradation. 65, 859-865.
540 [18] Mrozik, A., Miga, S., & Piotrowska-Seget, Z., 2011. Enhancement of
541 phenol degradation by soil bioaugmentation with Pseudomonas sp.
542 JS150. J. Appl. Microbiol. 111, 1357-1370.
543 [19] Westerholm, M., Levén, L., Schnürer, A., 2012. Bioaugmentation of
544 syntrophic acetate-oxidizing culture in biogas reactors exposed to
545 increasing levels of ammonia. Appl. Environ. Microbiol. 78, 7619-7625.
546 [20] Kumar, G., Bakonyi, P., Kobayashi, T., Xu, K. Q., Sivagurunathan, P.,
547 Kim, S. H., et al., 2016. Enhancement of biofuel production via microbial
548 augmentation: the case of dark fermentative hydrogen. Renew. Sust.
549 Energ. Rev. 57, 879-891.
550 [21] Wang, X., Feng, Y., Wang, H., Qu, Y., Yu, Y., Ren, N., et al., 2009.
551 Bioaugmentation for electricity generation from corn stover biomass
552 using microbial fuel cells. Environ. Sci. Technol. 43, 6088-6093.
553 [22] Raghavulu, S. V., Babu, P. S., Goud, R. K., Subhash, G. V., Srikanth,
554 S., Mohan, S. V., 2012. Bioaugmentation of an electrochemically active

555 strain to enhance the electron discharge of mixed culture: process
556 evaluation through electro-kinetic analysis. RSC Adv. 2, 677-688.
557 [23] Kiely, P. D., Regan, J. M., Logan, B. E., 2011. The electric picnic:
558 synergistic requirements for exoelectrogenic microbial
559 communities. Curr. Opin. Biotechnol. 22, 378-385.
560 [24] Raghavulu, S. V., Modestra, J. A., Amulya, K., Reddy, C. N., Mohan, S.
561 V., 2013. Relative effect of bioaugmentation with electrochemically
562 active and non-active bacteria on bioelectrogenesis in microbial fuel
563 cell. Bioresour. Technol. 146, 696-703.
564 [25] Wang, Y. F., Masuda, M., Tsujimura, S., Kano, K., 2008.
565 Electrochemical regulation of the end-product profile in
566 Propionibacterium freudenreichii ET-3 with an endogenous
567 mediator. Biotechnol. Bioeng. 101, 579-586.
568 [26] Mori, H., Sato, Y., Taketomo, N., Kamiyama, T., Yoshiyama, Y., Meguro,
569 S., et al., 1997. Isolation and structural identification of bifidogenic
570 growth stimulator produced by Propionibacterium freudenreichii. J. Dairy
571 Sci. 80, 1959-1964.
572 [27] Reiche, A., Sivell, J. L., Kirkwood, K. M., 2016. Electricity generation by
573 Propionibacterium freudenreichii in a mediatorless microbial fuel
574 cell. Biotechnol. Letters. 38, 51-55.
575 [28] Ledrich, M. L., Stemmler, S., Laval-Gilly, P., Foucaud, L., Falla, J., 2005.
576 Precipitation of silver-thiosulfate complex and immobilization of silver by
577 Cupriavidus metallidurans CH34. Biometals 18, 643-650.
578 [29] Monchy, S., Benotmane, M. A., Janssen, P., Vallaeys, T., Taghavi, S.,
579 van der Lelie, D., Mergeay, M., 2007. Plasmids pMOL28 and pMOL30 of
580 Cupriavidus metallidurans are specialized in the maximal viable
581 response to heavy metals. J. Bacteriol. 189, 7417-7425.
582 [30] Friman, H., Schechter, A., Nitzan, Y., Cahan, R., 2013. Phenol
583 degradation in bio-electrochemical cells. Int. Biodeterior. Biodegrad. 84,
584 155-160.

585 [31] Friman, H., Schechter, A., Ioffe, Y., Nitzan, Y., Cahan, R., 2013. Current
586 production in a microbial fuel cell using a pure culture of Cupriavidus
587 basilensis growing in acetate or phenol as a carbon source. Microb.
588 Biotechnol. 6, 425-434.
589 [32] Yamazaki, S. I., Kaneko, T., Taketomo, N., Kano, K., Ikeda, T., 2002.
590 Glucose metabolism of lactic acid bacteria changed by quinone-
591 mediated extracellular electron transfer. Biosci. Biotechnol. Biochem. 66,
592 2100-2106.
593 [33] Freguia, S., Masuda, M., Tsujimura, S., Kano, K., 2009. Lactococcus
594 lactis catalyses electricity generation at microbial fuel cell anodes via
595 excretion of a soluble quinone. Bioelectrochemistry 76, 14-18.
596 [34] Bakonyi, P., Koók, L., Keller, E., Bélafi-Bakó, K., Rózsenberszki, T.,
597 Saratale, G.D., et al., 2018. Development of bioelectrochemical systems
598 using various biogas fermenter effluents as inocula and municipal waste
599 liquor as adapting substrate. Bioresour. Technol. 259, 75-82.
600 [35] Rózsenberszki, T., Koók, L., Hutvágner, D., Nemestóthy, N., Bélafi-
601 Bakó, K., Bakonyi, P., et al., 2015. Comparison of anaerobic
602 degradation processes for bioenergy generation from liquid fraction of
603 pressed solid waste. Waste Biomass Valor. 6, 465-473.
604 [36] Zhen, G., Kobayashi, T., Lu, X., Kumar, G., Hu, Y., Bakonyi, P., et al.,
605 2016. Recovery of biohydrogen in a single-chamber microbial
606 electrohydrogenesis cell using liquid fraction of pressed municipal solid
607 waste (LPW) as substrate. Int. J. Hydrogen Energy 41, 17896-17906.
608 [37] Rózsenberszki, T., Koók, L., Bakonyi, P., Nemestóthy, N., Logroño, W.,
609 Pérez, M., et al., 2017. Municipal waste liquor treatment via
610 bioelectrochemical and fermentation (H_2 + CH_4) processes: Assessment
611 of various technological sequences. Chemosphere 171, 692-701.
612 [38] Koók, L., Nemestóthy, N., Bakonyi, P., Zhen, G., Kumar, G., Lu, X., et
613 al., 2017. Performance evaluation of microbial electrochemical systems
614 operated with Nafion and supported ionic liquid
615 membranes. Chemosphere 175, 350-355.

[39] Bakonyi, P., Borza, B., Orlovits, K., Simon, V., Nemestóthy, N., Bélafi-Bakó, K., 2014. Fermentative hydrogen production by conventionally and unconventionally heat pretreated seed cultures: A comparative assessment. Int. J. Hydrogen Energy 39, 5589-5596.

[40] Torres, C. I., Marcus, A. K., Lee, H. S., Parameswaran, P., Krajmalnik-Brown, R., Rittmann, B. E., 2009. A kinetic perspective on extracellular electron transfer by anode-respiring bacteria. FEMS Microbiol. Reviews 34, 3-17.

[41] Carmona-Martínez, A.A., Trably, E., Milferstedt, K., Lacroix, R., Etcheverry, L., Bernet, N., 2015. Long-term continuous operation of H_2 in microbial electrolysis cell (MEC) treating saline wastewater. Water Res. 81, 149-156.

[42] Rosenbaum, M. A., Bar, H. Y., Beg, Q. K., Segrè, D., Booth, J., Cotta, M. A., Angenent, L. T., 2011. Shewanella oneidensis in a lactate-fed pure-culture and a glucose-fed co-culture with Lactococcus lactis with an electrode as electron acceptor. Bioresour. Technol. 102, 2623-2628.

[43] Bae, W., Rittmann, B. E., 1996. Responses of intracellular cofactors to single and dual substrate limitations. Biotechnol. Bioeng. 49, 690-699.

[44] Mohanakrishna, G., Mohan, S. V., Sarma, P. N., 2010. Bio-electrochemical treatment of distillery wastewater in microbial fuel cell facilitating decolorization and desalination along with power generation. J. Hazard. Mater. 177, 487-494.

[45] Liu, H., Cheng, S., Logan, B. E., 2005. Production of electricity from acetate or butyrate using a single-chamber microbial fuel cell. Env. Sci. Technol. 39, 658-662.

[46] Kim, J. R., Jung, S. H., Regan, J. M., Logan, B. E., 2007. Electricity generation and microbial community analysis of alcohol powered microbial fuel cells. Bioresour. Technol. 98, 2568-2577.

[47] Torres, C. I., Marcus, A. K., Rittmann, B. E., 2007. Kinetics of consumption of fermentation products by anode-respiring bacteria. Appl. Microbiol. Biotechnol. 77, 689-697.

Table 1 – Stationary electric outputs and energy yield at different COD loadings for bioaugmented and control MFCs.

COD loading (g_{COD} L^{-1})		*Propionibacterium*-MFC	*Cupriavidus*-MFC	*Lactococcus*-MFC	Control-MFC
0.88		76.2 ± 1.98	70.6 ± 1.23	57.6 ± 3.61	66.2 ± 3.27
1.76	i_{max}	87.7 ± 2.46	81.3 ± 1.76	76.5 ± 1.37	80.2 ± 2.52
3.52	(mA m^{-2})	109.7 ± 0.86	95.8 ± 1.42	91.4 ± 1.98	92.3 ± 1.55
7.04		110.3 ± 0.76	100.1 ± 1.94	95.1 ± 1.55	102 ± 4.61
0.88		3.7 ± 0.18	3.2 ± 0.11	2.1 ± 0.24	2.8 ± 0.25
1.76	$P_{d,max}$	4.9 ± 0.26	4.2 ± 0.19	3.8 ± 0.13	4.1 ± 0.25
3.52	(mW m^{-2})	7.7 ± 0.12	5.9 ± 0.17	5.4 ± 0.22	5.5 ± 0.17
7.04		7.8 ± 0.13	6.4 ± 0.24	5.8 ± 0.18	6.7 ± 0.57
0.88		1.33 ± 0.05	1.54 ± 0.06	0.86 ± 0.04	1.45 ± 0.11
1.76	Y_S	1.19 ± 0.05	1.63 ± 0.09	1.15 ± 0.06	1.53 ± 0.17
3.52	(kJ $g_{\Delta COD}^{-1}$ m^{-2})	1.59 ± 0.09	1.62 ± 0.09	1.43 ± 0.09	1.69 ± 0.09
7.04		3.62 ± 0.20	2.29 ± 0.09	2.77 ± 0.16	1.89 ± 0.13

651 **Table 2 – Kinetic parameters and R-squared value of the fitted Monod**
652 **model.**

MFC type	i_{max} (mA m^{-2})	$K_{S,app}$ (e^- meq L^{-1})	R^2 (-)
Propionibacterium-MFC	120.5	67.7	0.988
Cupriavidus-MFC	111.1	73.5	0.999
Lactococcus-MFC	109.9	99.4	0.990
Control-MFC	112.4	91.0	0.988

653

654 Fig. 1

655

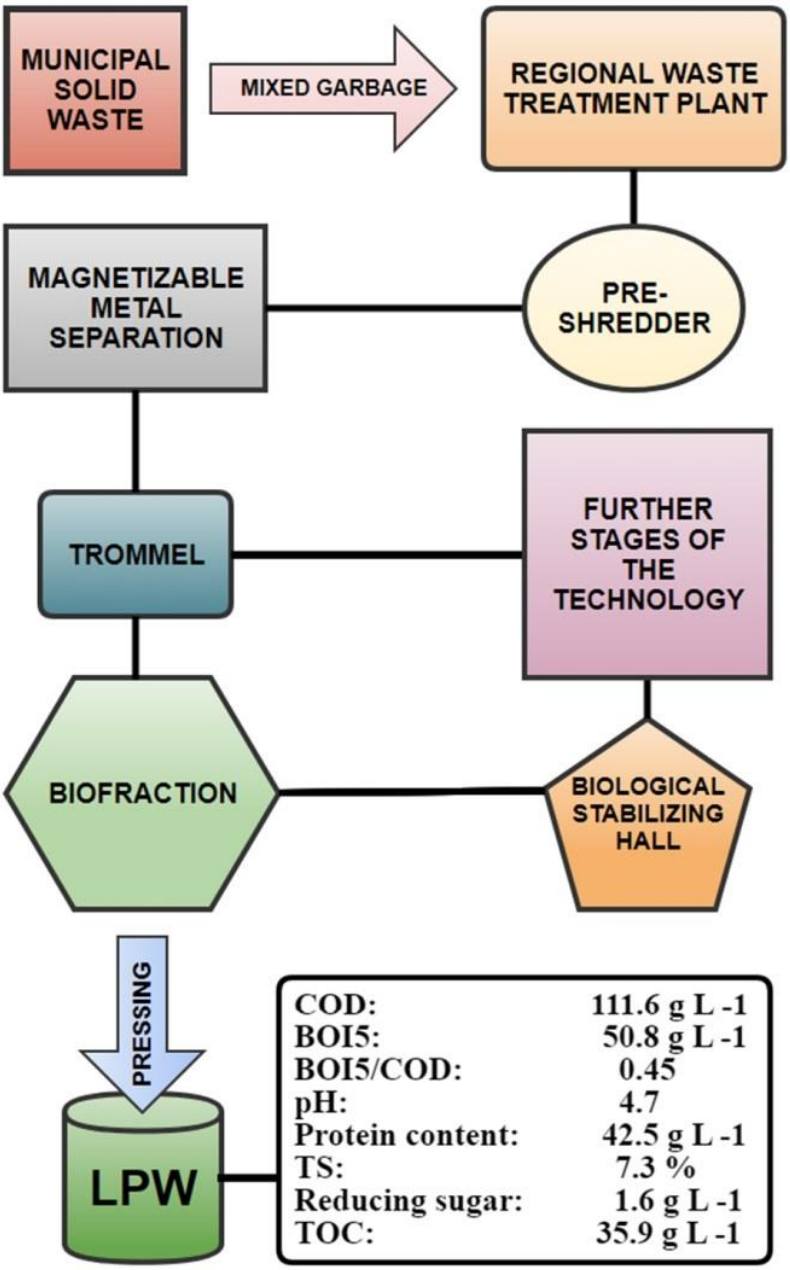

656

657

658 **Process flow diagram of LPW preparation.**

659

660

Fig. 2

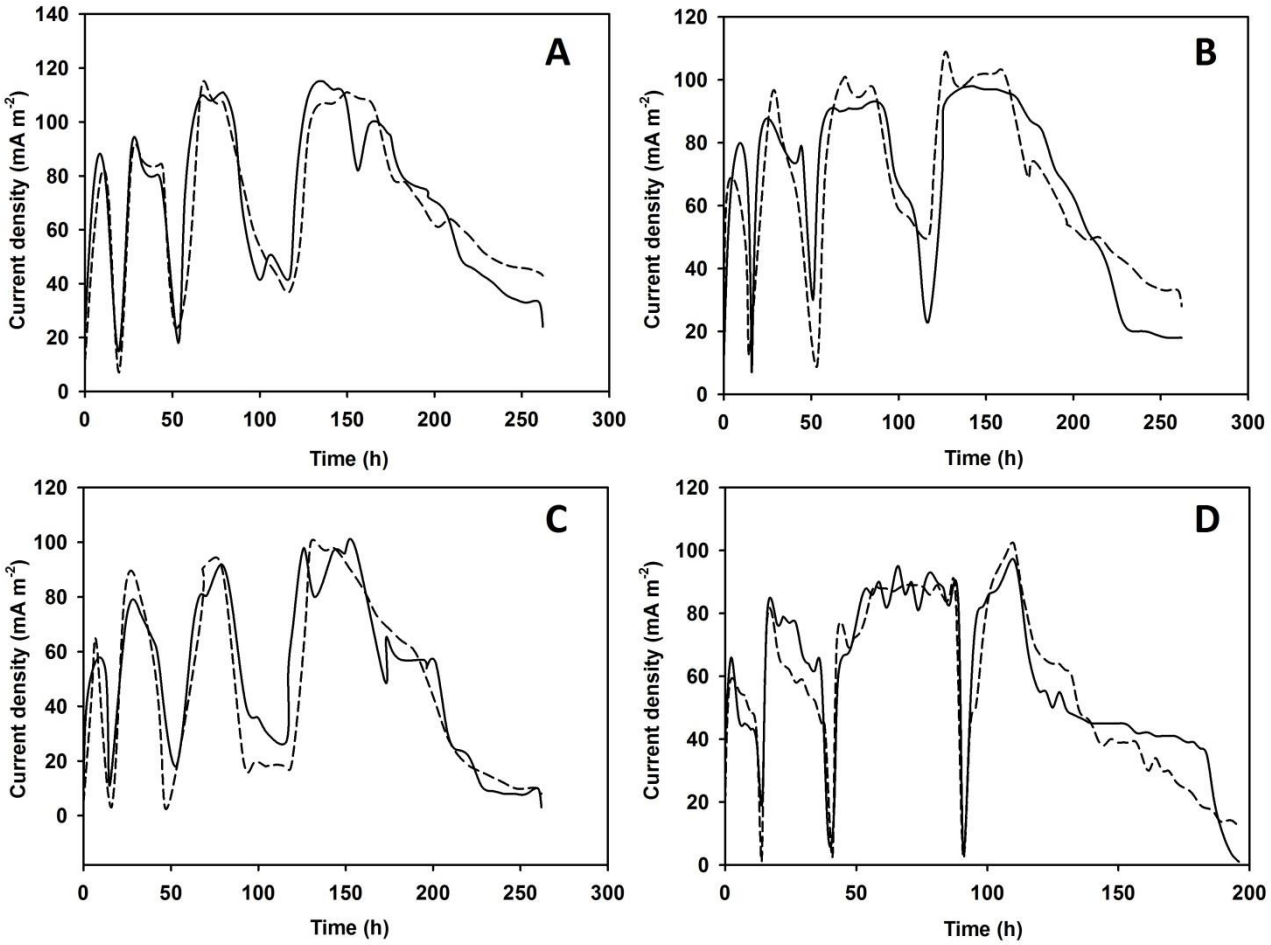

Current density profiles of the different MFCs (progress curves of replicates are shown). A: *Propionibacterium*-MFC; B: *Cupriavidus*-MFC; C: *Lactococcus*-MFC; D: Control-MFC. In all MFC, the order of substrate (LPW) loadings was the following: 0.5; 1; 2 and 4 mL.

670 Fig. 3

671

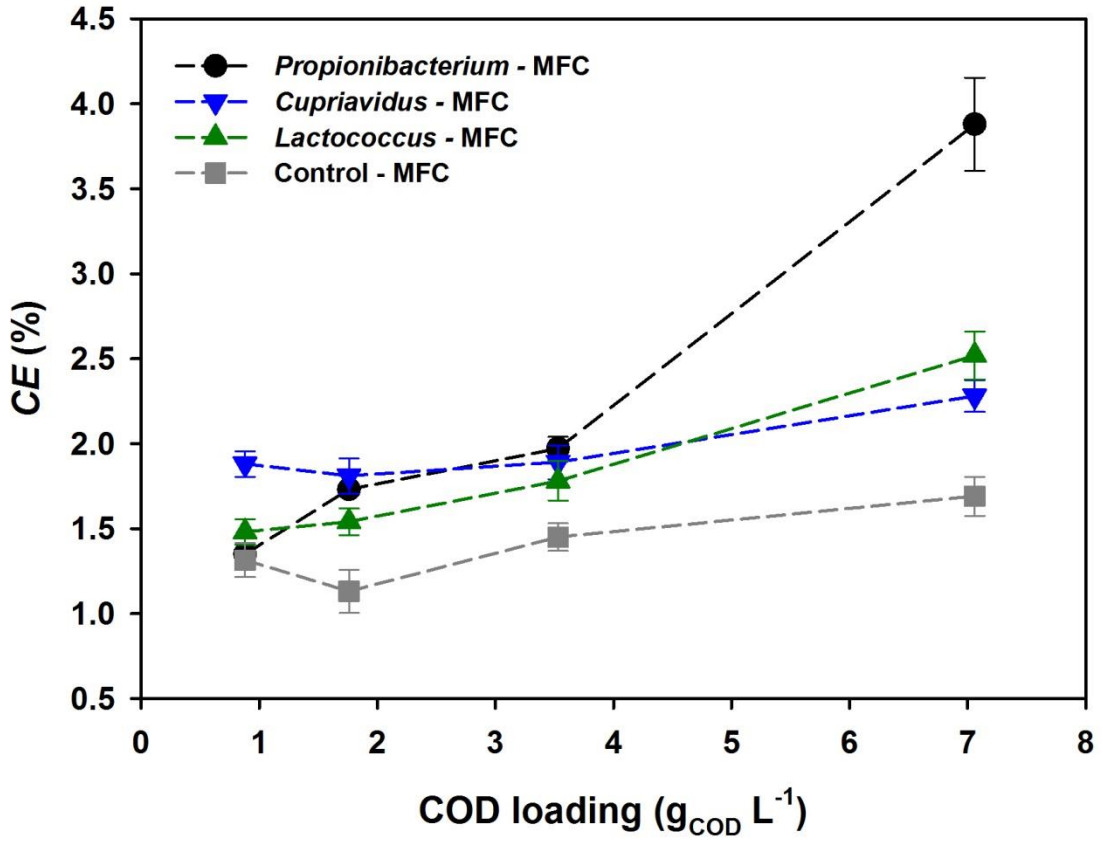

672

673

674 **Coulombic efficiency as a function of COD loading. -●-**: *Propionibacterium*-

675 MFC; -▼-: *Cupriavidus*-MFC; -▲-: *Lactococcus*-MFC; -■-: Control-MFC.

676

677

678 Fig. 4

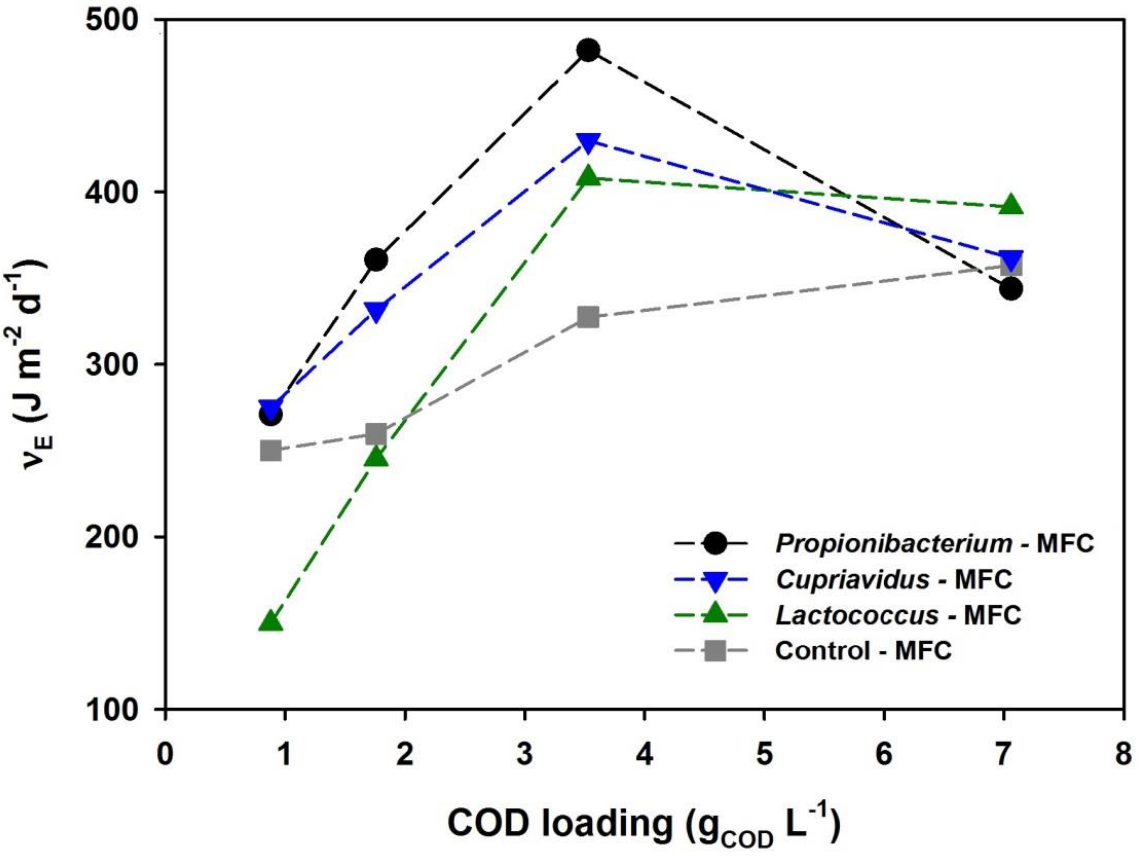

679

680

681 **Energy production rate of bioaugmented and control MFCs as a function**
682 **of COD loading. -●-**: *Propionibacterium*-MFC; **-▼-**: *Cupriavidus*-MFC; **-▲-**:
683 *Lactococcus*-MFC; **-■-**: Control-MFC.

684

685 Fig. 5

686

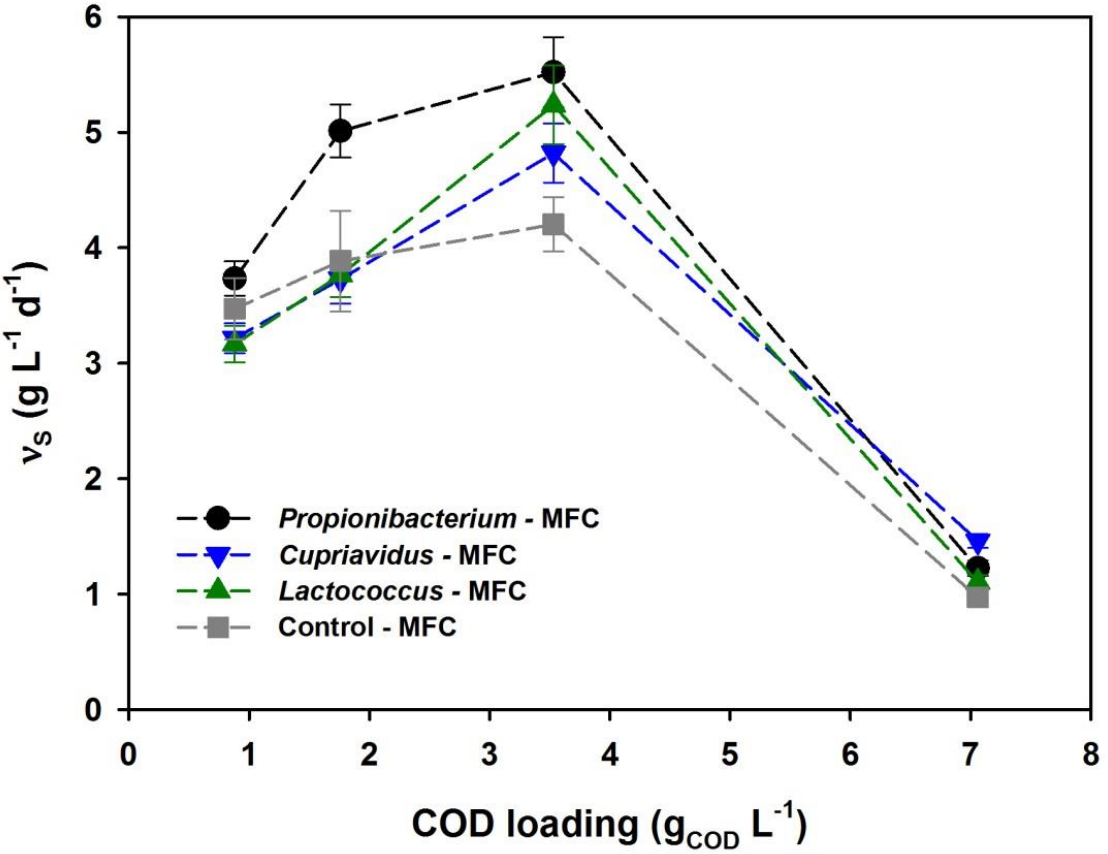

687

688

689 **COD removal rate of bioaugmented and control MFCs as a function of**
690 **COD loading. -●-**: *Propionibacterium*-MFC; **-▼-**: *Cupriavidus*-MFC; **-▲-**:
691 *Lactococcus*-MFC; -■-: Control-MFC.

692

693 Fig. 6

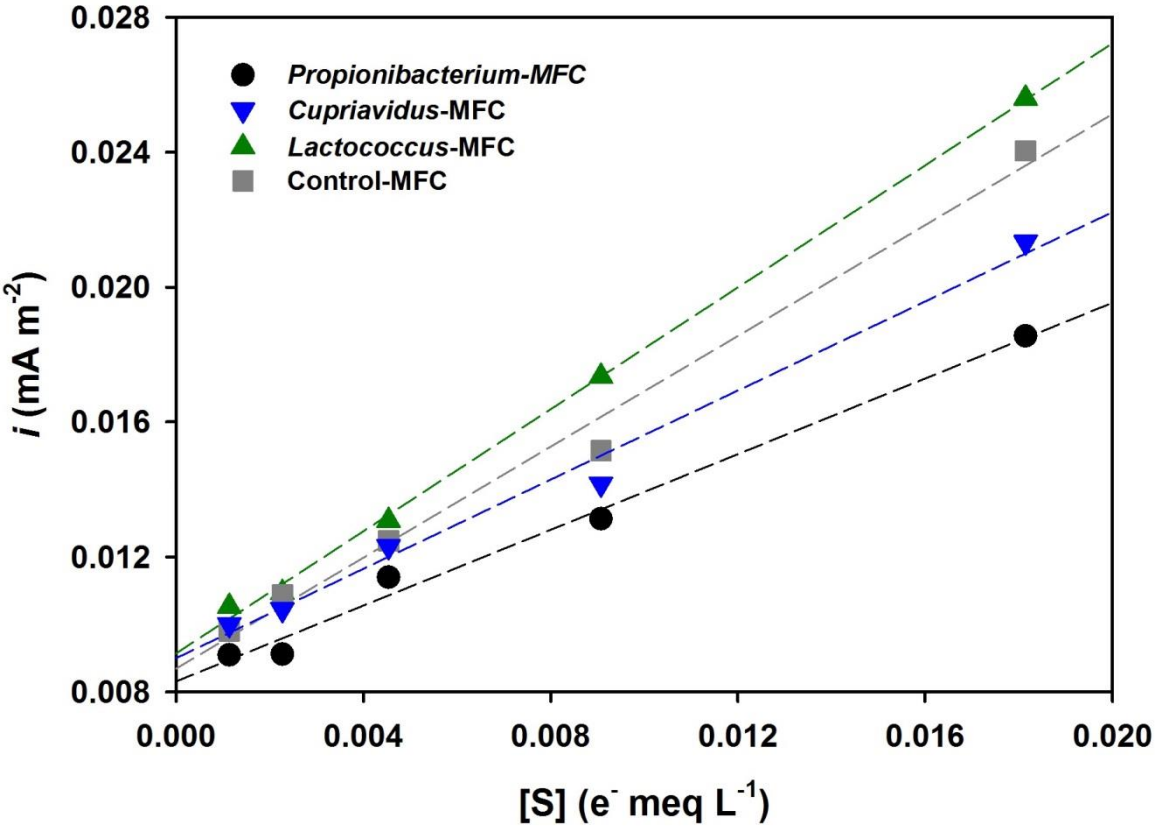

694

695

696 **Double-reciprocal plot of the Monod model for estimating the kinetic**

697 **parameters. -●-**: *Propionibacterium*-MFC; -▼-: *Cupriavidus*-MFC; -▲-:

698 *Lactococcus*-MFC; -■-: Control-MFC.

699

Fig. 7

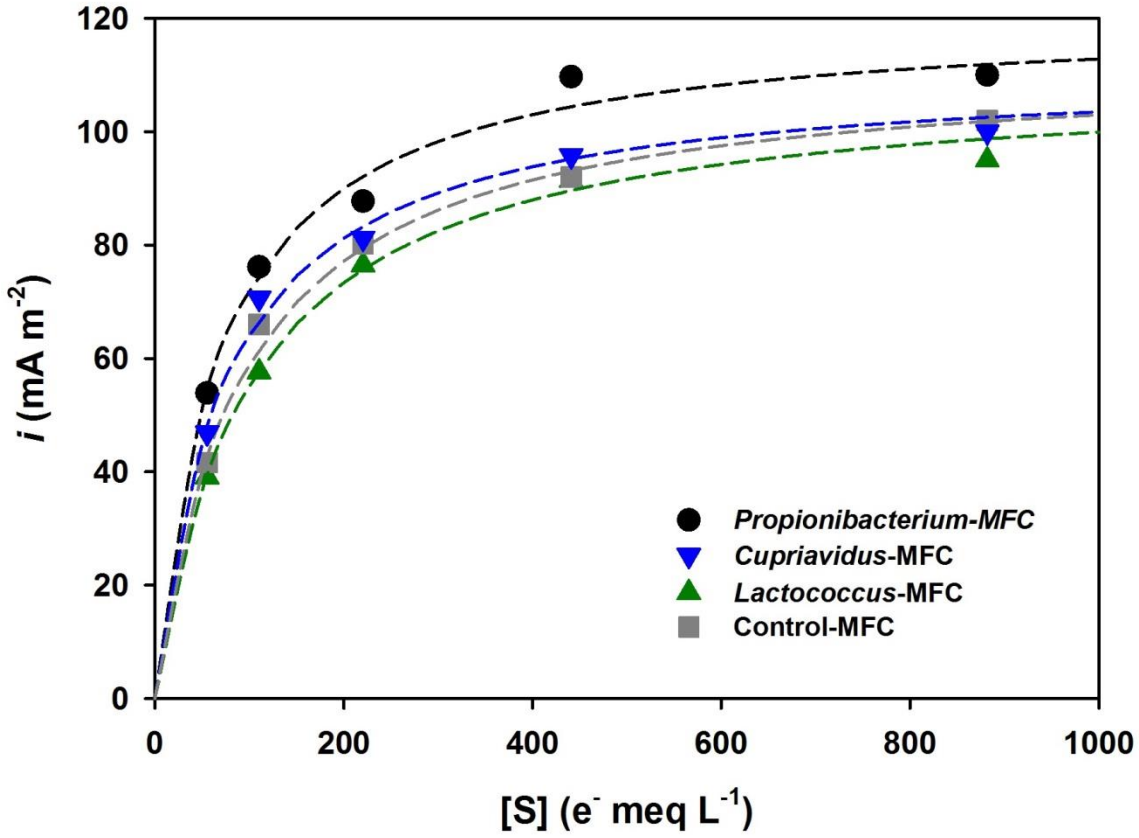

Monod kinetics of the bioaugmented and control MFCs. -●-: *Propionibacterium*-MFC; **-▼-**: *Cupriavidus*-MFC; **-▲-**: *Lactococcus*-MFC; **-■-**: Control-MFC.

Fig. 8

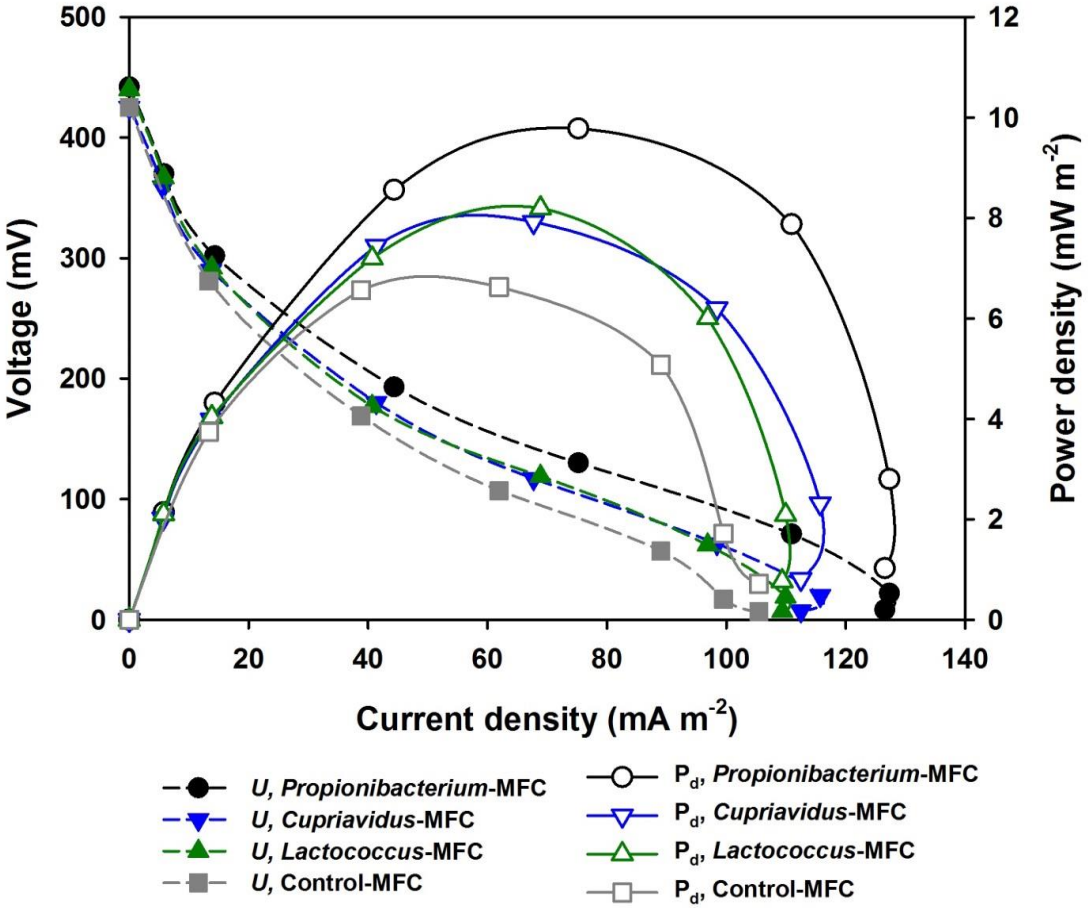

Polarization curves and power density plots for different MFCs. -●-: *U,* Propionibacterium-MFC; **-▼-**: *U, Cupriavidus*-MFC; **-▲-**: *U, Lactococcus*-MFC; **-■-**: *U,* Control-MFC; **-○-**: P_d, Propionibacterium-MFC; **-▽-**: P_d, *Cupriavidus*-MFC; **-Δ-**: P_d, *Lactococcus*-MFC; **-□-**: P_d, Control-MFC.